2023. – Vol. 461. – P. 01054. – URL: https://www.e3s-confere-nces.org/articles/e3sconf/abs/2023/ 98/e3sconf_rses23_ 01054/e3sc-onf_rses23_01054.html (дата обращения 13.05.2025).

12. Dielectric and microwave properties of ceramics of the Bi-Ti-O system / H. Sauchuk, N. Yurkevich, A. Akhmedov [et al.] // E3S Web of Conferences. – EDP Sciences, 2023. – Vol. 401. – P. 05076. – URL: https://www.e3s-conferences. org /articles/e3sconf/abs/2023/38/e3sconf_conmechydro23_05076/ e3sconf_con mechydro23_05076.html (дата обращения 10.04.2025).

13. Akhmedov, A. P. Innovative public transport stop with autonomous power supply / A. P. Akhmedov, S. B. Khudoyberganov, N. P. Yurkevich // Инновационные технологии в водном, коммунальном хозяйстве и водном транспорте : материалы Республиканской научно-технической конф., Минск, 20–21 мая 2021 г. / Белорусский национальный технический университет [и др.] ; редкол.: С. В. Харитончик [и др.]. – Минск, 2021. – С. 181–184.

УДК 620.9

Photovoltaic direct current power generation system

Abidova G. Sh., Kurbanov I. B.
Tashkent state transport university
Tashkent, Uzbekistan

The main source of energy for our planet is solar energy. It is the Sun that is the progenitor of all the main energy resources used by mankind – the Sun heats the atmosphere and the surface of the Earth, due to which winds blow, masses of water move, plants develop, organic fuels are formed. And in this regard, the potential of solar energy additionally provides such an opportunity as the use of solar energy to create alternative energy sources, and in this regard, the study of the properties of solar radiation is a particularly urgent task.

In this paper, a multiport dc-dc converter is proposed to be used as a converter. The three port converter contains three so called ports. Two are for solar panel and battery connection and the third one is for load connection.

The structural diagram of the autonomous solar-powered power supply system is shown in Fig. 1.

A multi-port converter has several advantages over stand-alone converters, such as fewer components, some circuit components are common to all ports. As a result, the system has a lighter weight and more compact assembly, which results in a lower cost of the inverter. In addition, there is no need to harmonize converters and transfer information between control systems.

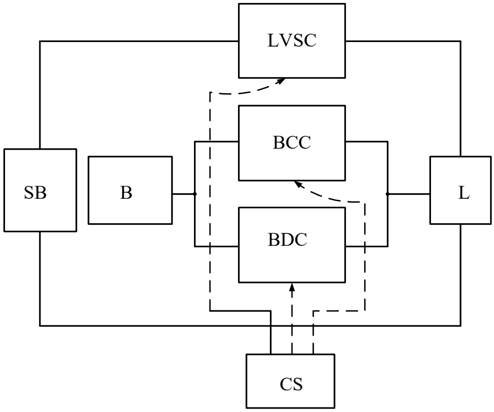

Fig. 1. Structural diagram of the autonomous power supply system:
SB – solar panel; *LVSC* – load voltage stabilization channel; *BCC* – battery charging channel; *BDC* – battery discharging channel; *B* – battery;
CS – control system; *L* – load

The proposed solar electric power conversion system contains a solar current control channel, a charging channel and a discharging channel of the battery pack. Thus, this circuit acts as a link between the solar panel and the battery pack, and increases the output voltage for further conversion in the AC link.

DC/DC converter. As a converter, a voltage regulator circuit is proposed in this paper to maintain the bus voltage at a fixed level. The schematic of the regulator is shown in Fig. 2.

The proposed power supply and energy conversion system contains a solar panel current regulator and battery charge-discharge regulators. Thus, this circuit acts as a link between the solar panel and the battery pack, and increases the output voltage for further conversion in the AC link.

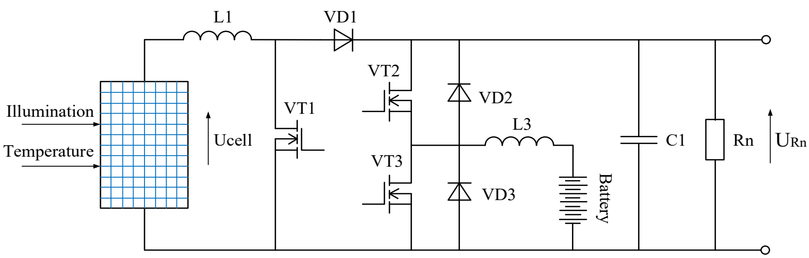

Fig. 2. DC/DC converter

The multiport inverter contains three so-called ports. Two are used to connect the solar and battery, and the third one is used to connect the load. Such a converter has a number of advantages over standard converters, such as fewer components because some circuit components are common to all ports, resulting in a system with a lower mass and more compact packaging, which provides a lower cost of the converter. In addition, there is no need to harmonize inverters and transfer information between control systems as it is often designed to be shared. This converter can operate in three channels depending on which transistor receives the control pulses.

Solar current channel. The substitution diagram (Fig. 3) represents a step-up converter. Consequently, the voltage at the load must be greater than the

voltage at the solar panel. The stabilizer is controlled by pulse width modulation. Control pulses are supplied to transistor *VT1*.

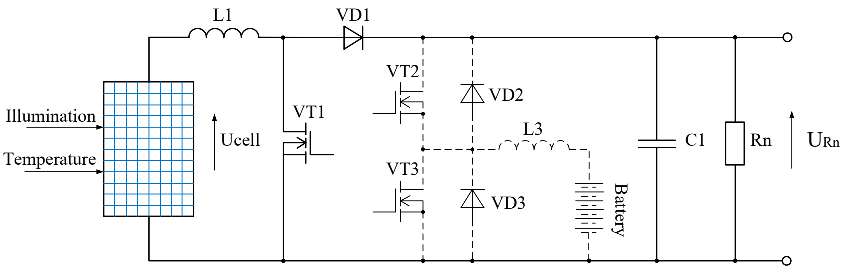

Fig. 3. Solar current regulator

This circuit contains two switching elements (*VT1*, *VD1*) and two reactive elements (*L1*, *C1*). During the interval of energy accumulation in the inductor, the transistor key is open, the solar battery voltage is applied to the inductor. During the accumulation interval, there is a linear rise of the inductance current from zero. At the same time, the diode is reverse energized and closed and the capacitance slowly discharges to the load. The energy storage and discharge intervals are described by the following system of equations:

$$\begin{cases} L\dfrac{di_L(t)}{dt} = U_C(t) \\ C\dfrac{dU_C(t)}{dt} = -\dfrac{U_C(t)}{R} \end{cases},$$

$$\begin{cases} L\dfrac{di_L(t)}{dt} - U_{in}(t) = -U_C(t) \\ i_L(t) - \dfrac{U_C(t)}{R} - C\dfrac{dU_C(t)}{dt} = 0 \end{cases},$$

where $L = L_1$; $C = C_1$; $U_{\text{in}} = U_{\text{cell}}$; $R = R_n$.

Battery charge channel. The charge controller, shown in Fig. 4, controls charge battery in the mode of varying, depending on the level of illumination, the current while maintaining the voltage at the load. Commutation of transistor VT2 regulates the current flowing into the battery.

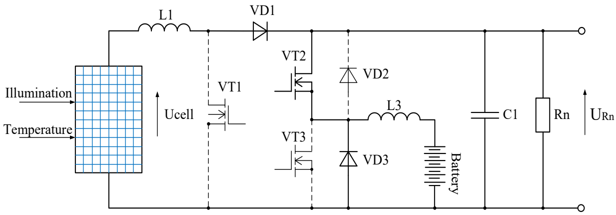

Fig. 4. Battery charge regulator

The charging current decreases as the charge accumulates, thus avoiding the accumulation of gas in the storage cells, which in turn increases their lifetime. Thus, the operation of the charge controller is similar to that of a stabilizer, and all the excess energy produced by the solar panel is stored in the storage battery, leading to an increase in the efficiency of the system as a whole. The conversion stages are described by the following systems of equations:

$$\begin{cases} L\dfrac{di_{L2}(t)}{dt} = -U_{\text{АКБ}}(t) \\ L\dfrac{di_{L1}(t)}{dt} + U_{in}(t) = -U_C(t) \\ i_L(t) - C\dfrac{dU_C(t)}{dt} - \dfrac{U_C(t)}{R} = 0 \end{cases},$$

Battery discharge channel. The charge controller (Fig. 5), is a converter, which increases the voltage received from the battery to the load voltage by switching the *VT3* switch.

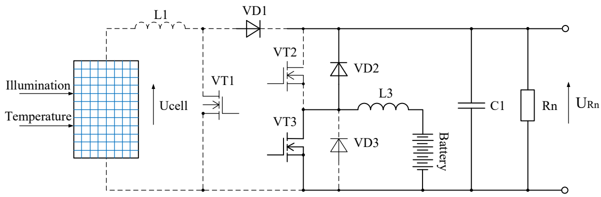

Fig. 5. Battery discharge regulator

The voltage from the battery, as in the case of the solar current channel, is boosted to the required level and stabilized at the load by storing energy in an inductance and switching the power switch. These processes are described by the following system of equations

$$\begin{cases} L\dfrac{di_{L2}(t)}{dt} - U_{\text{АКБ}}(t) = -U_C(t) \\ i_{L2}(t) - \dfrac{U_C(t)}{R} - C\dfrac{dU_C(t)}{dt} = 0 \end{cases},$$

where $L = L_2$; $C = C_1$; $U_{\text{in}} = U_{\text{cell}}$; $R = R_n$.

Setting up a neural network for the inverter. Despite the advantages of a three-port inverter, it is necessary to ensure timely switching between the operating channels. Consequently, the design of the control system becomes the most challenging task.

The main component of such a control system will be the unit that ensures that the inverter operates at the maximum power point, i.e. the control system must work in conjunction with the maximum power point tracking algorithm.

Since solar panel characteristics are non-linear and maximum power can only be achieved at one point. In order to extract maximum power from PV panels, regardless of weather conditions and load size, it is necessary to operate at the maximum power point to maximize energy efficiency. Consequently, a control system that provides a maximum power point tracking function for all levels of solar irradiation becomes a key device for the successful operation of off-grid systems. Since solar cell characteristics are non-linear and maximum power can only be achieved at a single point. To extract maximum power from PV panels, regardless of weather conditions and load, it is necessary to operate at the point of maximum power to maximize energy efficiency. Therefore, a control system that provides the function of tracking the maximum power point for all levels of solar irradiation becomes a key device for the successful operation of off-grid systems.

The neural network contains an input layer, two hidden layers and one output layer. The input data of the network are: illuminance, temperature, voltage and current of the solar module. The signal of the output neuron is equal to the voltage at which the maximum power of the solar module is reached. Fig. 6 shows the overall architecture of the ANN that was used in the initial setup of the control system to simplify the task of control signal generation.

But, as it was described earlier, the use of such a neural network in the control system implies the use of additional sensors. To a greater extent, this concerns the use of illumination sensors. Since the illumination must be determined accurately enough for the system to work properly, there must be a sufficient number of sensors installed in the correct position. Faced with this problem, attempts have been made to do away with the illuminance sensor. Short circuit current has a proportional dependence on illumination, it can be assumed that the solar panel current data will be sufficient for correct operation of the ANN.

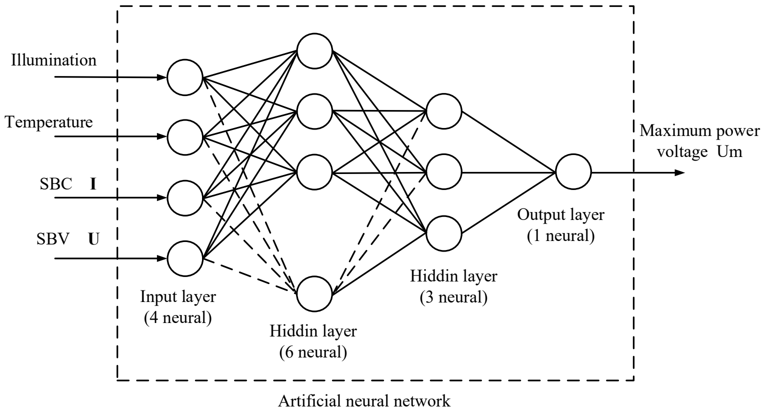

Fig. 6. Topology of artificial neural network

Thus, according to the improved methodology of ANN creation and training, only the values of temperature, voltage, and current of the solar panel are input to the neural network. Some problems encountered in the previous study were avoided by increasing the amount of training data and increasing the number of neurons in hidden layers. The architecture of the developed neural network is presented in Fig. 7.

Structure of the management system. For effective operation of the converter, it is necessary to ensure that the maximum power of the solar panel is taken away during operation of any of the channels. Depending on the converter channel, the operation of the control system was divided into modes depending on the operating conditions of the autonomous system as a whole. The operating conditions of the autonomous system are: daytime, when the solar panel produces enough energy to supply the load; evening or cloudy time, when solar energy is insufficient to supply the load with the required amount of energy; dark time of day, when the solar panel does not produce energy.

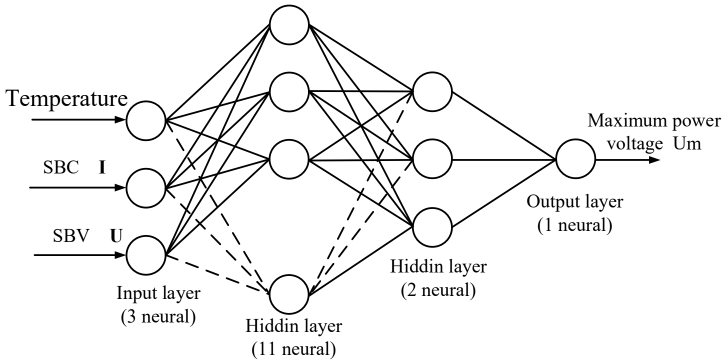

Fig. 7. Topology of artificial neural network

Based on these conditions, four modes of operation can be distinguished:

1. The first mode is to find the point of maximum power of the solar panel and stabilization of the voltage at the load. The artificial neural network is used to estimate how much energy from the solar panel remains unused and whether a battery can be connected.

2. f there is an excess of energy from the solar panel, this system allows you to «give» part of the energy to the battery by connecting the battery charging channel. The control system, guided by the data received from the INS, ensures a smooth transition from mode 1 to mode 2 so that no voltage sags occur at the load when the battery is connected. The energy priority remains with the load, and the excess energy from the solar panel is stored in the battery.

3. In the event that the illumination starts to decrease, the control system, receiving a task signal from the artificial neural network, gradually reduces the charging current of the battery to avoid overvoltage on the load. In this case, the maximum power is drawn from the solar panel, and the lack of energy is replenished by the battery.

4. The battery provides the load with stabilized voltage at the required level. The simplified structure of the developed control system is shown Fig. 8.

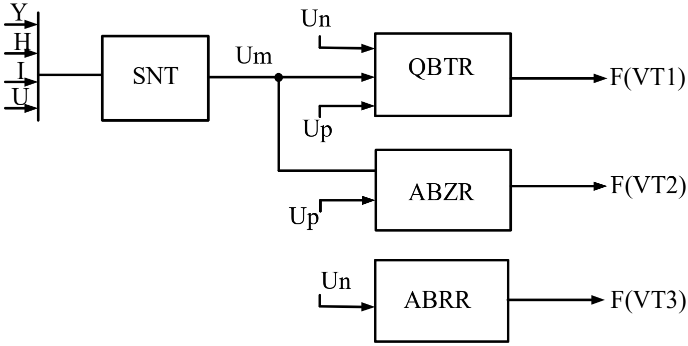

Fig. 8. Structure of the multiport converter control system direct current

Simulation model. The power circuit model and intelligent control system implemented on Matlab software elements are shown in Fig. 9–10.

There are several main blocks in the control system:

1. Artificial neural network block. ANN provides the mode tracking the maximum power point. The network input receives signals corresponding to the conditions in which the solar module is located: temperature, solar radiation, current and voltage at the output terminals of the solar module. The neural network generates two signals: a voltage signal corresponding to the maximum power voltage and a signal of the difference between the voltage at the maximum power point and the actual maximum power voltage of the solar panel.

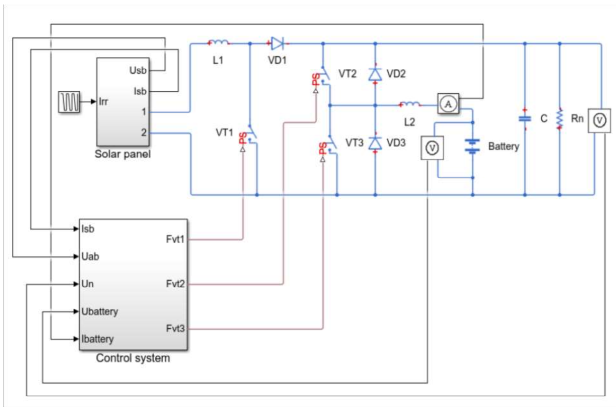

Fig. 9. Power circuit diagram of the converter

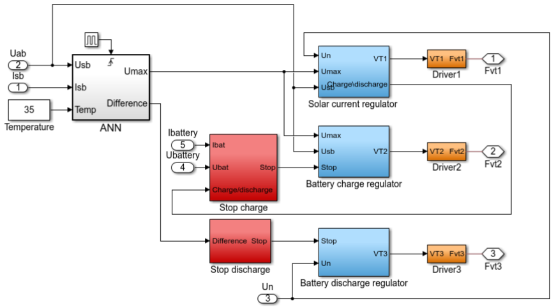

Fig. 10. Intelligent control system

2. Current regulator SB. This block compares the signal of the INS with the solar battery voltage and determines the operation mode of the circuit. Next, the PWM block generates control pulses that are fed to transistor *VT1*.

3. Battery charge regulator. Comparing the voltage of the solar panel with the voltage of the maximum power of the INS, the PWM generates control pulses of transistor VT2, storing the excess energy of the SB into the battery.

4. Battery discharge regulator. Performs the function of voltage stabilization on the load when powered by the battery.

5. There are also charge and discharge prohibition blocks in the control system, providing protection against overcharging or complete discharge of the battery, which significantly extends the life of the battery.

The current and voltage diagrams for the main operating modes of the circuit are given as the results of numerical experiment.

Fig. 11 shows the time diagrams of input and output voltages and battery current. These conditions correspond to the illumination level E = 50,0 W/m, temperature T = 35 ^oC.

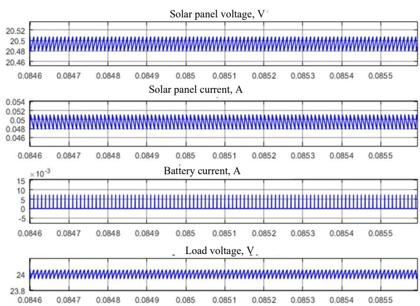

Fig. 11. the time diagrams of input and output voltages and battery current

Analyzing the obtained graphs, it can be stated that this illumination is sufficient to stabilize the voltage at 24 *V*. Excess energy is stored in the accumulator battery. the supply voltage received from the output of the neural network is UMPPT = 20,32 *V*. In this case, the steady-state voltage at the solar panel is U_{sb} = 20,49 *V*. Thus, the system draws maximum energy from the solar panel with an accuracy of 99,2 %.

References

1. Investigation of solar absorber for small scale solar concentrating parabolic dish / B. M. Habtamu, V. Trygve, L. Jorgen [et al.] // ISES Solar World Congress : proceeding, Kassel, German, 28 Aug.–2 Sept. 2011. – Kassel, 2011. – P. 2616–2623.

2. Безруких, П. П. Возобновляемая энергетика как стимул развития электротехнической промышленности / П. П. Безруких // Электро. – 2010. – № 1. – С. 9–14.

3. Smith, R. Poised for Growth / R. Smith, L. Lohn // Sun and Wind Energy. 2009. – № 6. – P. 74–78.

4. Study on the biparametrical transudations circuits with distributed parameters / S. F. Amirov, A. Kh. Sulliev, A. T. Sanbetova [et al.] // IOP Conf. Series: Earth and Environmental Science. – 2021. – Vol. 939. – P. 012008. – doi:10.1088/1755-1315/939/1/012008.

5. Boltayev, O. T. Consideration of the nonlinearity of the magnetization curve in the Calculation of magnetic chains with a moving electromagnetic screen / O. T. Boltayev, F. A. Akhmedova, I. B. Kurbanov // Universum: tekhnicheskie nauki. – 2022. – Vol. 95, № 2. – URL: https://7universum.com/ru/tech/archive/item/13086 (дата обращения: 14.06.2025).

6. Abidova, G. Sh. Analysis and selection of the type of analogue-digital converter used in the processing of informational data / G. Sh. Abidova, G. R. Qahharova, I. B. Kurbanov // Материалы 66-й Международной научной конференции Астраханского государственного технического университета, Астрахань, 25–29 апр. 2022. – Астрахань, 2022. – С. 367–370.

7. On the Perturband-Observe and Incremental Conductance MPPT Methods for PV Systems / D. Sera, L. Mathe, T. Kerekes [et al.] // IEEE J. Photovolt. – 2013. – Vol. 3, № 3. – P. 1070–1078.

8. Dielectric and microwave properties of ceramics of the Bi-Ti-O system / H. Sauchuk, N. Yurkevich, A. Akhmedov [et al.] // E3S Web of Conferences. – EDP Sciences, 2023. – Vol. 401. – P. 05076. – URL: https://www.e3s-conferences. org /articles/e3sconf/abs/2023/38/e3sconf_conmechydro23_05076/ e3sconf_con mechydro23_05076.html (дата обращения 10.04.2025).

9. Zhang, N. A review of topologies of three-port DC–DC converters for the integration of renewable energy and energy storage system / N. Zhang, D. Sutanto // Renew. Sustain. Energy Rev. – 2016. – Vol. 56. – P. 388–401.

10. Kabir E. Solar energy: Potential and future prospects / E. Kabir, P. Kumar, S. Kumar, A. A. Adelodun, K.-H. Kim // Renew. Sustain. Energy Rev. – 2018. – Vol. 82. – P. 894–900.

УДК 622.631.6

Ветровые эрозионные процессы в Ахалском велаяте Туркменистана

Мыратбердиев Я., Аманов М. Э., Тайлиев Я. Г., Годыков П. Е.
Туркменский государственный архитектурно-строительный институт
Ашгабат, Туркменистан

В Ахалском велаяте при совместном влиянии антропогенных и природных факторов деструктивные процессы в почвах связаны, прежде всего, с развитием ветровой эрозии почв. Среди климатических факторов, способствующих развитию эрозии почв, основными являются: температура воздуха, количество и интенсивность осадков, а также скорость и направление ветров.

В разных природных зонах климатические характеристики могут существенно отличаться, что определяет преимущественное развитие ветровой эрозии почв. Это необходимо учитывать при организации системы противоэрозионных мероприятий в регионе. Ветровая эрозия возникает на больших территориях и загрязняет окружающую природную среду атмосферы и гидросферы [1–3].

Таблица 1

Значения средних месячных и годовых температур воздуха t, ^{0}C и осадков, мм

Месяцы	1	2	3	4	5	6	В год
t,C^0	0,6	3,9	7,4	16,2	23,3	27,0	
Осадки, мм	24	32	43	30	25	19	
Месяцы	7	8	9	10	11	12	
t, C^0	30,5	29,2	21,9	16,4	12,5	2,8	16, 2
Осадки, мм	6	2	3	11	17	16	228

На рис. 1 показана повторяемость (%) направлений ветра за год.